Horizontal Discretization and Forcing

by
Zaviša I. Janjić, Fedor Mesinger
(University of Belgrade, Yugoslavia)
and
Thomas L. Black*
(National Meteorological Center, Washington)

1. Introduction

This presentation addresses two problems. The first one is that of the response of the flow simulated by finite-difference models to small scale forcing. The second problem is related to the treatment of topographical forcing, and, in particular, the choice of the vertical coordinate.

1.1. Small scale forcing

After the pioneering work of Winninghoff (1968) and Arakawa (1970; also Arakawa and Lamb 1977) it has become clear that various rectangular horizontal grids are not offering the same advantages for the simulation of large- and synoptic-scale atmospheric motions. Additional arguments have been summarized by Mesinger (1981), and by Janjić and Mesinger (1984). The evidence accumulated so far strongly suggests that, with presently available finite-difference schemes, the non-staggered, and the staggered D grid should not be used. The remaining two possibilities are the staggered C grid and the semi-staggered B/E grid.

In simulation of the geostrophic adjustment process, the B/E grid has a grid-separation problem with the short waves, particularly in the case of the external and the lower internal modes. However, a technique has been developed (Mesinger 1973; Janjić 1974, 1979), which to a large extent overcomes the problem (Vasiljević 1982; Cullen 1983; Janjić and Mesinger 1984).

The C grid, on the other hand, has a difficulty with higher internal modes, but for <u>all</u> wave lengths. These modes are present in models with currently used vertical resolutions and it is not known whether something can be done about this problem.

---

* Lecture presented by Z.I. Janjić

For simulation of the slowly changing quasi-geostrophic motion, horizontal advection schemes which strictly control nonlinear energy cascade towards smaller scales have been developed for both the C and the E grid (Arakawa and Lamb 1981; Janjić 1984). However, not all of the conservation properties of the two schemes are the same. Among the differences, the C grid scheme conserves potential enstrophy, while the E grid scheme conserves momentum, and imposes a more stringent constraint on the false cascade of energy towards smaller scales. Thus, on balance, properties of the E grid scheme do not appear inferior, and may be superior, to those of the C grid scheme.

Finally, a recent study of Dragosavac and Janjić (1987) shows that, with currently used horizontal resolutions, the linear amplitude response of the centered B/E grid schemes to forcing by topography may be generally more accurate than that of the C grid schemes. Thus, according to this study, the B/E grid may be advantageous for the simulation of the steady solutions induced by topography, even on the synoptic scale.

The present considerations are devoted to a further study of the properties of the staggered C grid and the semi-staggered E/B grid. Namely, in case of a small-scale forcing, convergence properties of simplest second-order finite-difference schemes are examined in a series of numerical experiments with varying resolution. On the E grid, the modification preventing grid separation is applied.

1.2. Vertical coordinate and horizontal discretization

The σ system has become popular because of its simple lower boundary condition and a straightforward formal horizontal discretization. However, the σ coordinate is known to have difficulties in the presence of steep topography. These difficulties are not restricted to the pressure gradient force error; problems are encountered also with lateral diffusion and horizontal advection (see e.g. the review paper by Mesinger and Janjić, 1987). With increased horizontal resolution these difficulties will not disappear. On the contrary, they can be expected to become more serious since better resolution of the model topography results in generally higher and steeper mountains.

Notwithstanding the sizable theoretical evidence, the effects of the σ coordinate problems have been difficult to demonstrate clearly and convincingly in comprehensive atmospheric models. The reason for this has been either the lack of competitive reference forecasts produced using an alternative discretization technique, or the uncertainties concerning the

representativeness of the results due to the differences in the formulations of the models which have been compared.

As an alternative to the σ coordinate, considered to be better suited for higher horizontal and vertical resolutions, a blocking technique with step-like mountain representation has been recently proposed (Mesinger, 1984). Being a generalized form of the σ coordinate, Mesinger's η coordinate allows the same model to be run either in the σ or in the η mode. Thus, in addition to its other possible advantages, an η coordinate model can be used as a tool for closer inspection of the properties of the σ coordinate by making parallel runs in the σ and the η modes.

If the undesirable effects of the σ coordinate problems can be convincingly demonstrated, and, as the consequence, the decision is made to abandon the terrain following coordinates, the alternative technique for the representation of mountains is likely to require reformulation of the horizontal discretization technique. For example, if a blocking technique is applied, the problem of the internal boundaries is introduced. This problem has been successfuly solved in an η coordinate grid point model (Mesinger et al., 1987; Mesinger and Janjić, 1987). It is not obvious, however, whether, and if so, how this can be done in a spectral model.

In this presentation an attempt will be made to find out whether, as the theoretical evidence is suggesting, the horizontal resolutions have been reached at which the alternatives to the σ coordinate should be taken into consideration. In order to do so, the preliminary results will be discussed of recent parallel experiments in the η and the σ mode (Black and Janjić, 1988) using a comprehensive high resolution limited area model (Mesinger et al., 1987; Janjić and Black, 1987).

II. *Small-scale forcing on the semi-staggered E/B and the staggered C grid: convergence properties and implications for the parameterization problem*

II.1. Design and results of experiments

The same experiment design has been adopted as that of the early "source-sink" experiments of Arakawa (1972) and Mesinger (1973). Namely, the shallow water equations were integrated in a rectangular domain. The size of the integration domain was 5250 km by 3500 km in the case of the C grid, and 5303.30 km by 3535.53 km in the case of the E grid. The slight

difference between the sizes of the integration domains is due to the different geometry of the two grids and the requirement that the dimensions of the two domains be as close as possible, with the grid distance the same in both cases.

The mean height of the free surface of the fluid H was 1000 m and the Coriolis parameter f was assumed to be 0.0001 s^{-1}. The gravity g was 9.80 m s^{-2}. No slip boundary conditions were used. A source and a sink, 1750 km apart on the C grid, and 1767.77 km apart on the E grid, were placed symmetrically in the central part of the domain along a line oriented in the east-west direction. The intensities of both source and sink were 2 m min^{-1}.

The lowest resolution experiment was performed with the grid distance d=250 km. The experiments were then repeated with 125 km and 62.5 km mesh size. In the pair of experiments with the lowest resolution, the source and the sink were restricted to single grid points. In the 125 km experiments, the source and the sink consisted of four grid points each, with equal intensity of forcing at each of the four points. Analogously, in the 62.5 km experiments, there were 16 points with equal intensity of forcing at both source and sink. Since the integration domains of the higher resolution experiments were of the same sizes as those of the lowest resolution experiments, the centers of these higher resolution source and sink areas had to be shifted slightly with respect to their lowest resolution symmetrical positions. They were shifted toward northwest for the C grid experiments, and toward west for the E grid experiments; by $\sqrt{2}d/2$ and by $\sqrt{2}d/4$ in case of the medium resolution and in case of the highest resolution experiments, respectively.

Forward-backward time-integration scheme was used for the gravity wave terms, and the simplest forward scheme was applied for Coriolis and advection terms in the equations of motion. The time steps chosen for the integrations on the E grid were 30, 15 and 7.5 min, depending on the resolution used. These values represented about 0.71 of the maximum time steps allowed by the CFL criterion for the forward-backward scheme for the gravity-wave part of the equations. The E grid results discussed in this section were obtained using the modification with the weighting factor w=0.25. One may recall (e.g. Janjić, 1979) that with w not exceeding this value, the maximum time step allowed by the CFL criterion is not reduced. In the case of the C grid, depending on the resolution, the time steps were 20, 10 and 5 min. Note that, with equal spatial resolution, the C grid requires shorter time step than the E/B grid due to more accurate differencing in the pressure gradient force and divergence terms.

As to remaining space differencing, the simplest centered schemes were used, with differencing performed in between the nearest points carrying the same variable, and averaging as appropriate.

The diagrams displayed in Fig. II.1 represent the height of the free surface at the sink point after 24 hours of forcing in the case of 250 km experiments, and the height averaged over four and sixteen forced sink points in the cases of 125 km and 62.5 km experiments. The dots on the light and the heavy solid lines correspond to the results obtained on the C and on the E grid, respectively. As can be inferred from the figure, the solutions on both grids converge with about equal rapidity. However, the C grid tends to underestimate the value of height at the sink, while the reverse is true for the E grid. Thus, the solutions on the two grids converge approaching the true solution from different sides.

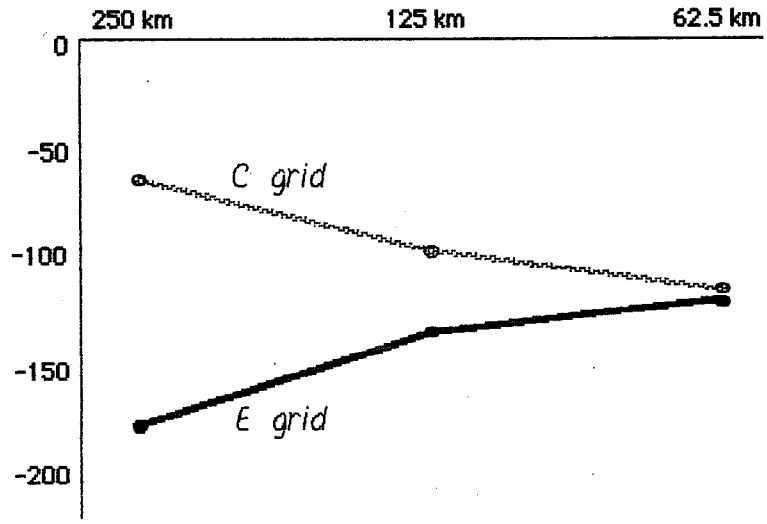

Fig. II.1. Height at the sink point after 24 hours of forcing in the case of 250 km experiments, and the height averaged over four and sixteen forced sink points in the cases of 125 km and 62.5 km resolutions for the grid C (dots connected by light solid line), and the grid E (dots connected by heavy solid line).

This result is consistent with what should be expected from the geostrophic adjustment theory when applied to the spatially discretized systems. Namely, in the case of linearized shallow water equations on an f-plane, if a disturbance is introduced in the height field, the ratio of the amplitude of the wave solution corresponding to the geostrophic part, G_g, and

the amplitude of the wave component of the initial disturbance, G_0, are given by

$$G_g/G_0 = f^2/[f^2+gH(k^2+l^2)]$$

(see e.g. Janjić and Wiin-Nielsen 1977; Daley 1980). Here, k and l are the wave number vector components, and the other symbols used have already been defined. Due to averaging of the Coriolis force term, on the C grid the analog of the numerator tends to zero as the shortest resolvable scale is approached. Therefore, the amplitudes of the geostrophic part of the solution will be underestimated. Specifically, for the shortest resolvable scale the amplitude of the geostrophic part will be equal to zero. For this scale only the gravity waves can exist. On the other hand, as the shortest resolvable wave is approached on the E grid without modification, the analog of the term $gH(k^2+l^2)$ appearing in the denominator, tends to zero. Thus, the amplitudes of the geostrophic part of the solution are overestimated. In particular, for the shortest resolvable scale, the amplitude of the geostrophic part will be equal to the amplitude of the initial disturbance.

On the E grid, the overestimation of the depth at the sink is related to the separation of solutions. With the forward-backward scheme, the continuity equation modified to prevent the separation of solutions (Janjić 1979, Eq. 26) is

$$h^{\tau+1}=h^{\tau}-\Delta t\nabla_{+\cdot}(h^{*}\mathbf{v})^{\tau}+(\Delta t)^2wgH(\nabla^2_x-\nabla^2_+)h^{\tau}. \qquad (II.1)$$

Here τ and $\tau+1$ denote the time levels; Δt is the time step, h^* the value of h at a velocity point whatever its definition may be, $\mathbf{v}$ the velocity vector, and $\nabla_{+\cdot}$ as well as ∇^2_x and ∇^2_+ are the finite-difference analogs of the $\nabla\cdot$ and the ∇^2 operator, respectively, calculated using the nearest values located in the directions indicated by the subscripts. With the modification term in (II.1) of a higher order in Δt than the mass divergence term, the total effect of the modification in a given finite interval of time will depend on the value of the time step. This being noted, one might suspect that the modification in performed experiments has not been entirely successful in eliminating the separation of solutions on the two C sub-grids. Namely, the time step was only about 0.71 of the maximum time step allowed by the CFL criterion for the gravity-wave part of the equations.

II.2. The effect of the modification on convergence

As pointed out, the efficiency of the modification depends on the ratio of the actually used time step and the maximum allowed time step by the CFL stability criterion. The larger the time step used, the more efficient the modification should be. This situation is illustrated in Fig. II.2, showing the height at the sink point after 24 hours in the 250 km resolution experiment as a function of time step. Indeed, with small time steps, the depth at the sink point is found to be about twice that of the true solution, presumably very nearly equal to these of the two highest resolution experiments shown in Fig. II.1.

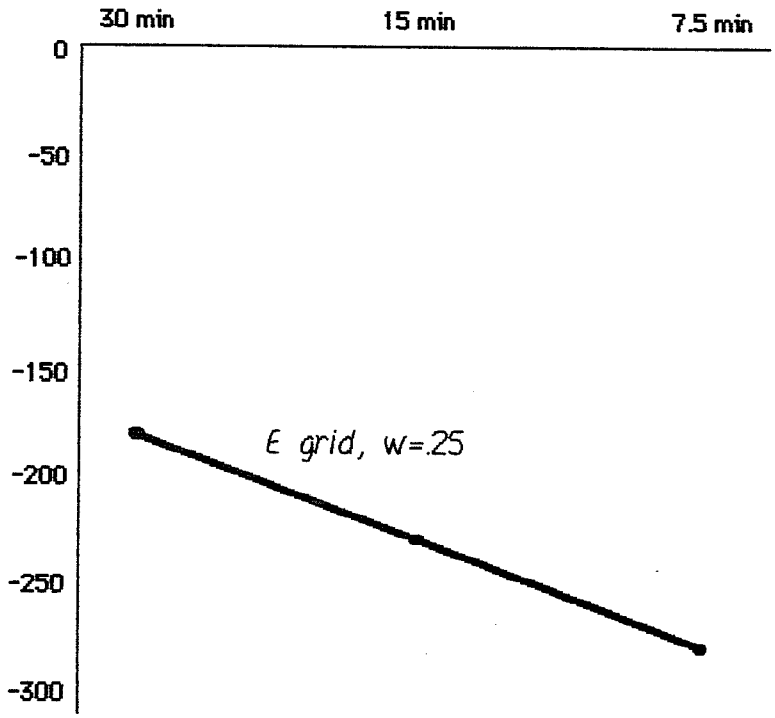

Fig. II.2. Height at the sink point (heavy dots) after 24 hours in the 250 km resolution experiment as a function of time step.

In experiments illustrated in Fig. II.2, this perhaps unattractive dependence of the effect of the modification on the time step can of course be removed by increasing the weight of the modification with decreasing time step. An issue of a more general interest is that of a possibility for achieving a faster convergence with given, and not unnecessarily small time steps, such as those used for experiments of Fig. II.1.

The modification has been introduced on the basis of purely physical arguments (Mesinger 1973, 1974; Janjić 1974, 1979). However, an alternative approach, which sheds new light on the nature of the modification, may also be convenient. Namely, at the beginning of the time step in between the time levels τ and $\tau+1$, the starting value of height $h^{\tau*}$ at a grid point, can be defined as a linear combination of the value of height at that grid point, and the value h'^{τ} obtained by fourth order interpolation from the surrounding eight points, i.e.

$$h^{\tau*}=\alpha h^{\tau}+(1-\alpha)h'^{\tau}.$$

Using the notation of grid points introduced in Fig. II.3, after some algebra,

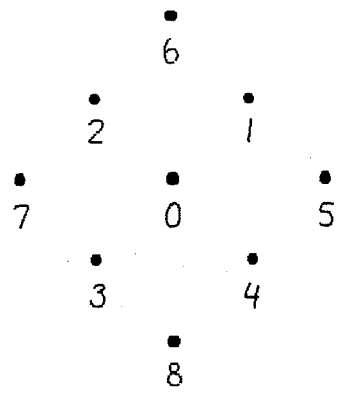

Fig. II.3. Stencil and notation of the grid points used in the discussion of the modification term.

one obtains

$$h_0^{\tau*}=\alpha h_0^{\tau}+(1-\alpha)\{h_0+(1/2)[(h_1+h_2+h_3+h_4-4h_0)-(1/2)(h_5+h_6+h_7+h_8-4h_0)]\}^{\tau}$$

or,

$$h_0^{\tau*}=h_0^{\tau}+[(1-\alpha)/2][(h_1+h_2+h_3+h_4-4h_0)-(1/2)(h_5+h_6+h_7+h_8-4h_0)]^{\tau}.$$

On the right hand side of the last equation we recognize the modification

term of Eq. (1) with the factor $wgH(\Delta t/d)^2$ replaced by $(1-\alpha)/2$. If we choose $\alpha=1/2$, the factor $(1-\alpha)/2$ takes on the value 1/4 which corresponds to the modification applied with w=0.25 for the maximum time step allowed by the CFL stability criterion. In other words, with $\alpha=1/2$ the modification will have its maximum weight permitted for stability. With w=1/4, it has had its maximum weight permitted not to affect the CFL condition of the gravity-wave part of the equations.

To check the effect of an increased weight of modification on convergence, the E grid experiments of Section II.2 were repeated with $\alpha=1/2$. The results obtained are indicated by the dots on the heavy solid line in Fig. II.4. The results obtained with w=0.25, already shown in Fig.II.1, are also displayed in this figure for comparison (dots on the light solid line).

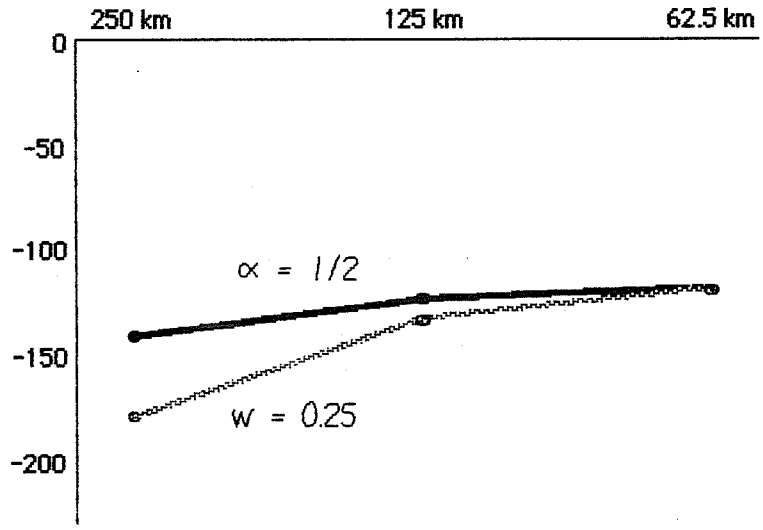

Fig. II.4. Height at the sink point after 24 hours of forcing in the case of 250 km experiments, and the height averaged over four and sixteen forced sink points in the cases of 125 km and 62.5 km resolutions for the weight of the modification which is maximum permitted for stability (dots connected by heavy solid line), and for the weight which is maximum not to affect the CFL stability condition with the parameters chosen as in the experiments shown in Fig. 1 (dots connected by light solid line).

Apparently, with $\alpha=1/2$, the situation has improved considerably, the convergence being accelerated by approximately a factor of two, which coincides with the increase of the actual weight of the modification. The

results of the E grid experiments are now clearly better than those on the C grid.

III. Vertical coordinate and horizontal discretization

III.1 The model

a. The vertical coordinate

The HIBU+ (Hydrometeorological Institute and Belgrade University + GFDL, NMC and NCAR/UCAR) limited area model was used in the experiments. The model uses the so called η vertical coordinate (Mesinger, 1984) defined by

$$\eta=[(p-p_T)/(p_S-p_T)]\eta_S \; ; \; \eta_S=[p_{rf}(z_S)-p_T]/[p_{rf}(0)-p_T] \; .$$

Here, p is pressure, the subscripts S and T denote the values at the bottom and at the top of the model's atmosphere respectively, z is the geometrical height, and p_{rf} is the reference pressure depending only on height. Normally, with this coordinate the mountains are represented as steps shown schematically in Fig. III.1, and the flow is blocked at the vertical sides of

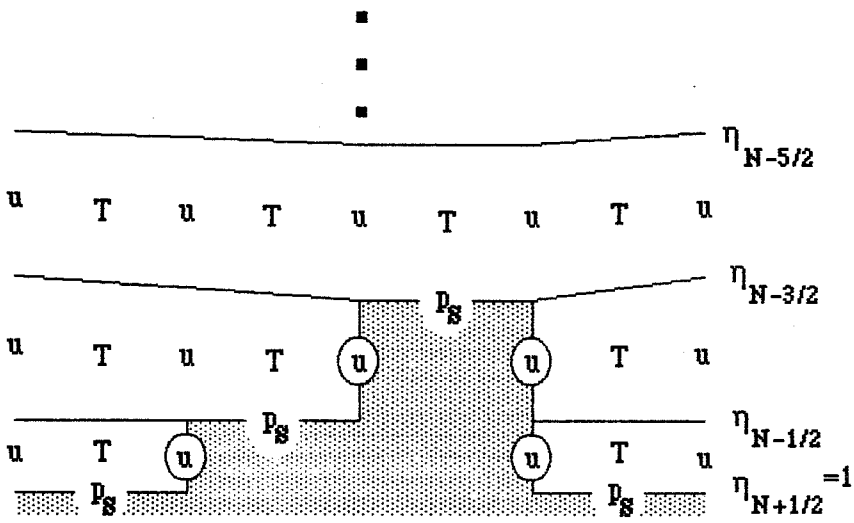

Fig. III.1. Schematic representation of the step-mountain η vertical coordinate.

the steps. However, as can be seen from the definition, the η coordinate degenerates into one of the commonly used forms of the σ coordinate if η_s is set to unity everywhere. Thus, in order to compare the two vertical discretization techniques, the same model can be run in either the η or the σ mode.

b. The dynamical part

The highlights of the design of the dynamical part of the model have already been reported at the ECMWF seminars (e.g. Mesinger and Janjić, 1987). It will suffice to say here that the model is defined on the semi-staggered Arakawa E grid, the technique for preventing elementary grid separation (Mesinger, 1973) is used in combination with the split explicit time differencing scheme (Janjić, 1979), the horizontal advection scheme has a built-in strict nonlinear energy cascade control (Janjić, 1984), the technique used for the treatment of the internal boundary conditions preserves all major properties of the horizontal advection schemes (Mesinger and Janjić, 1987; Mesinger et al., 1987), the model vectorizes well and executes efficiently (Mesinger and Janjić, 1987; Mesinger et al., 1987).

c. The physical package

A comprehensive physical package has been recently incorporated in the model (Janjić and Black, 1987). The package consists of the Mellor-Yamada Level 2.5 scheme (Zilitinkevitch, 1970; Mellor and Yamada 1974; Mellor and Yamada, 1982), the Mellor-Yamada Level 2 scheme for the "surface" layer (Mellor and Yamada, 1974, 1982) with a dynamical turbulence layer which is currently 2 metres deep, surface processes, fourth order lateral diffusion scheme with the diffusion coefficient depending on deformation and the turbulent kinetic energy, large scale precipitation, Betts and Miller shallow and deep convection schemes (Betts, 1986; Betts and Miller, 1986) and the NMC version of the GLA radiation scheme with interactive random overlap clouds (Davies, 1982; Harshvaradhan and Corsetti, 1984).

d. The computational problem of the Level 2.5 turbulence closure model

It should be noted that a severe computational problem may be encountered with the Level 2.5 closure model if the time differencing scheme for the turbulent kinetic energy generation/dissipation terms is not carefully designed. Namely, if the closure model is implemented in the split mode, starting from the Mellor and Yamada Eq. (36) (1982), the equation describing the time evolution of the square root of the turbulent kinetic

energy due to the turbulent energy generation/dissipation may be written in the form

$$\partial q/\partial t = Aq^2.$$

Here, the expression A may be either positive or negative and varies in magnitude depending on the stability and shear, and in an implicit way on the turbulent kinetic energy. In the time stepping procedure we shall calculate it diagnostically at the beginning of the time step Δt. Thus, if the backward time differencing scheme is used, we obtain

$$q^{\tau+1} = q^{\tau} + A^{\tau}\,\Delta t\,(q^{\tau+1})^2 .$$

This is a quadratic equation for $q^{\tau+1}$ with the roots

$$q_1^{\tau+1} = (1 - \sqrt{1-4A^{\tau}\Delta t q^{\tau}})/(2A^{\tau}\Delta t),$$

$$q_2^{\tau+1} = (1 + \sqrt{1-4A^{\tau}\Delta t q^{\tau}})/(2A^{\tau}\Delta t).$$

When $\Delta t \to 0$, $q_1^{\tau+1} \to q^{\tau}$, and, therefore, q_1 is the physical solution. The other solution is computational and should be removed. However, this is not enough to provide stable integrations with conveniently chosen Δt. Namely, unless Δt is kept small, the expression under the square root sign may become negative. Thus, as the split prognostic equation for the turbulent kinetic energy generation/dissipation, we are using

$$(q^{\tau+1})^2 = [(1 - \sqrt{1-4A^{\tau}\Delta t q^{\tau}})/(2A^{\tau}\Delta t q^{\tau})]^2\,(q^{\tau})^2,$$
$$\text{if } 1-4A^{\tau}\Delta t q^{\tau} \geq 0;$$

$$\text{and} \qquad (3.1)$$

$$(q^{\tau+1})^2 = [1/(2A^{\tau}\Delta t q^{\tau})]^2\,(q^{\tau})^2,$$
$$\text{if } 1-4A^{\tau}\Delta t q^{\tau} < 0.$$

By doing so, we are not imposing any artificial constraint on the turbulent kinetic energy itself. Instead, as can be easily verified from (3.1), the growth rate of the turbulent kinetic energy is limited, so that $(q^{\tau+1})^2$ can not exceed $4(q^{\tau})^2$. In a way, this can be compared to commonly used procedures

for slowing down processes which are too fast for the time resolution used, such as e.g. polar filtering, or implied deceleration of the gravity waves associated with the application of the semi-implicit scheme.

With the current implementation, the elimination of the described problem was essential in order to get the Level 2.5 model working. Moreover, with the time differencing technique (3.1), the turbulent kinetic energy adjusts quickly to the forcing irrespectively of the initial conditions, and behaves well, staying within the bounds expected from physical considerations.

e. Efficiency

With about 8500 grid points in the horizontal, 15 layers in the vertical, and the horizontal resolution of about 80 km, the model requires about 500 CPU seconds per day on the CYBER 205. Out of these, the dynamical part takes about 180 CPU seconds, the physical package excluding radiation about 120 CPU seconds, and the radiation takes about 200 seconds. It is interesting to note that the Level 2.5 turbulence closure model is computationally remarkably inexpensive. It required less CPU time than the previously used dry convective adjustment procedure and a very simple turbulent momentum transport scheme.

III.2 The experiments

A sequence of 48 hour real data forecasts were run by Black (Black and Janjić, 1988) both in the η and in the σ mode starting from 13 consecutive observational times in late August this year. The integration domain covered Eastern Pacific, North American continent and Western Atlantic. The vertical and the horizontal resolutions were as described before. The initial conditions were interpolated to the model grid using the archived NMC data on standard pressure levels. The NMC global aviation forecasts were used to specify the boundary conditions.

a. Noise

As already reported at the ECMWF seminars by Mesinger and Janjić (1987) (see also Mesinger, 1985), in the early experiments with the "minimum physics" version of the η coordinate model, it was noticed that when the model was run in the σ mode, a much higher level of noise was produced than in the η mode. This remained generally true as the new physical parameterization schemes were being incorporated in the model.

b. Precipitation

Special attention was paid to precipitation which was believed to be most sensitive and difficult to predict. The precipitation forecasts were verified using threat and bias scores. The accumulated 24 hour precipitation was used as the verification variable. The verification area extended over larger part of the United States. The scores were calculated on the grid of the NMC's so called Limited Area Fine Mesh model (LFM) with horizontal resolution of 190.5 km at 60 degrees north. The model produced precipitation was interpolated from the model grid to the LFM grid using bilinear interpolation. The actual precipitation data, in the original form gridded on a finer grid, were averaged over LFM grid boxes to produce the verification fields. The two procedures used to define the forecast and the verification data on the LFM grid are obviously inconsistent and may have affected the scores. However, the scores were calculated in exactly the same way for both the η and the σ forecasts, and therefore they could still be considered as at least partly relevant in relative terms.

The scores were calculated separately for 0-24, 12-36 and 24-48 hr forecasts. Average scores for all 13 cases and for all forecast times are shown in Table 2.1. Winning scores are printed in boldface. As can be seen

Amounts (inches)	Threat		Bias	
	σ	η	σ	η
0.01	0.364	**0.412**	0.712	**0.802**
0.25	0.139	**0.197**	0.869	**0.950**
0.50	0.080	**0.156**	**1.213**	1.374
0.75	0.060	**0.131**	**1.374**	1.679
1.00	0.049	**0.121**	**1.491**	1.821
1.25	0.036	**0.110**	**1.515**	2.265
1.50	0.038	**0.114**	**1.422**	2.467
1.75	0.031	**0.122**	**1.750**	2.833
2.00	0.0	**0.095**	**1.476**	2.286
2.50	0.0	0.0	**2.167**	2.833

Table 2.1 Average precipitation scores for all forecast times in 13 parallel 48 hour runs in the σ and the η mode. The winning scores are printed in boldface.

from the table, the model systematically produced significantly better threat scores in the η mode. On the other hand, the bias scores were generally closer to unity in the σ runs. However, considering the inconsistent interpolations involved, the significance of the latter in absolute terms is not quite clear.

c. Mean height error

The mean height error was examined because of the radiation scheme employed. Namely, the same radiation scheme is used in the NMC's Regional Area Forecasting System (RAFS), and this scheme was believed to be responsible for the cold bias present in this system.

The mean height error averaged over the sequence of 13 forecasts showed that the η model was cooling as well. However, the absolute value of the maximum error at the end of the 48 hr forecast period was about one third of that of RAFS. Moreover, inspection of some individual cases showed that the η model was occasionally producing positive mean height errors which never occurred in the sample of RAFS forecasts.

Perhaps the most surprising result was that the absolute value of the mean height error increased about twice when the HIBU+ model was rerun in the σ mode. In some individual cases the mean height error patterns in the σ mode showed striking similarity to those of RAFS. Two such cases are shown in Figs. III.2 and III.3. In the figures, the RAFS mean height error as a function of pressure and forecast period is shown in the upper left panel. The HIBU+ errors obtained in the σ mode runs are shown in the lower left panel. The errors of the HIBU+ runs in the η mode are shown in the lower right panel.

Although the sample considered is relatively short, and the similarity of the error patterns of the σ coordinate runs was not as pronounced in all individual cases as in the two cases shown here, the sensitivity of the HIBU+ model to changing the vertical coordinate from η to σ was strong and systematic, resulting on the average in about twice larger absolute values of the error at the end of the forecast period in the σ mode. This result was, in a way, reconfirmed by comparison with the RAFS forecasts. However, the exact mechanism of the error growth in the σ coordinate remains unknown.

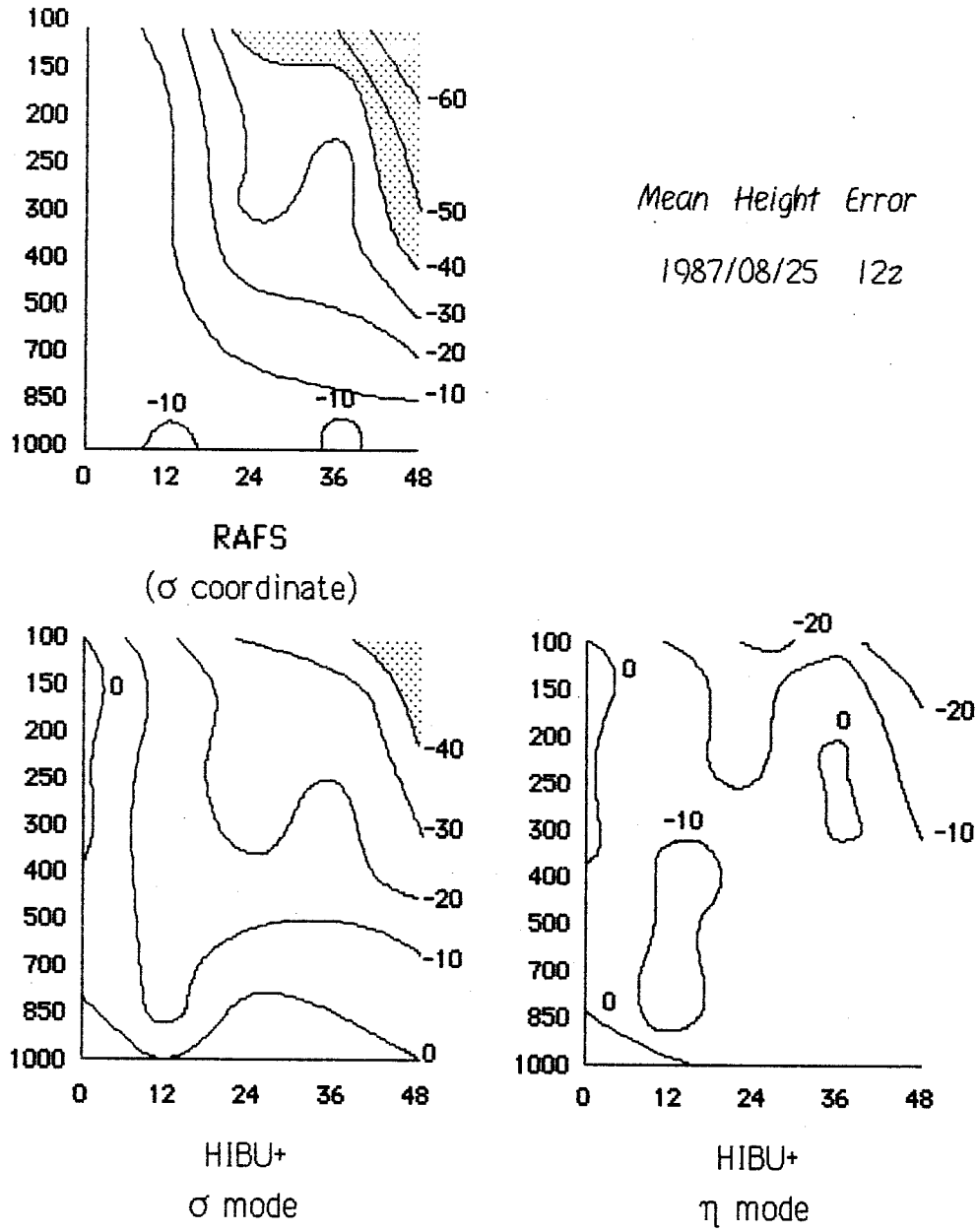

Fig. III.2. Mean height error of the 48 hour forecast starting from August 25, 1987, 12Z obtained with RAFS (upper panel), the HIBU+ model run in the σ mode (lower left panel), and, the HIBU+ model run in the η mode (lower right panel). The area in which the error exceeds 40 metres is shaded.

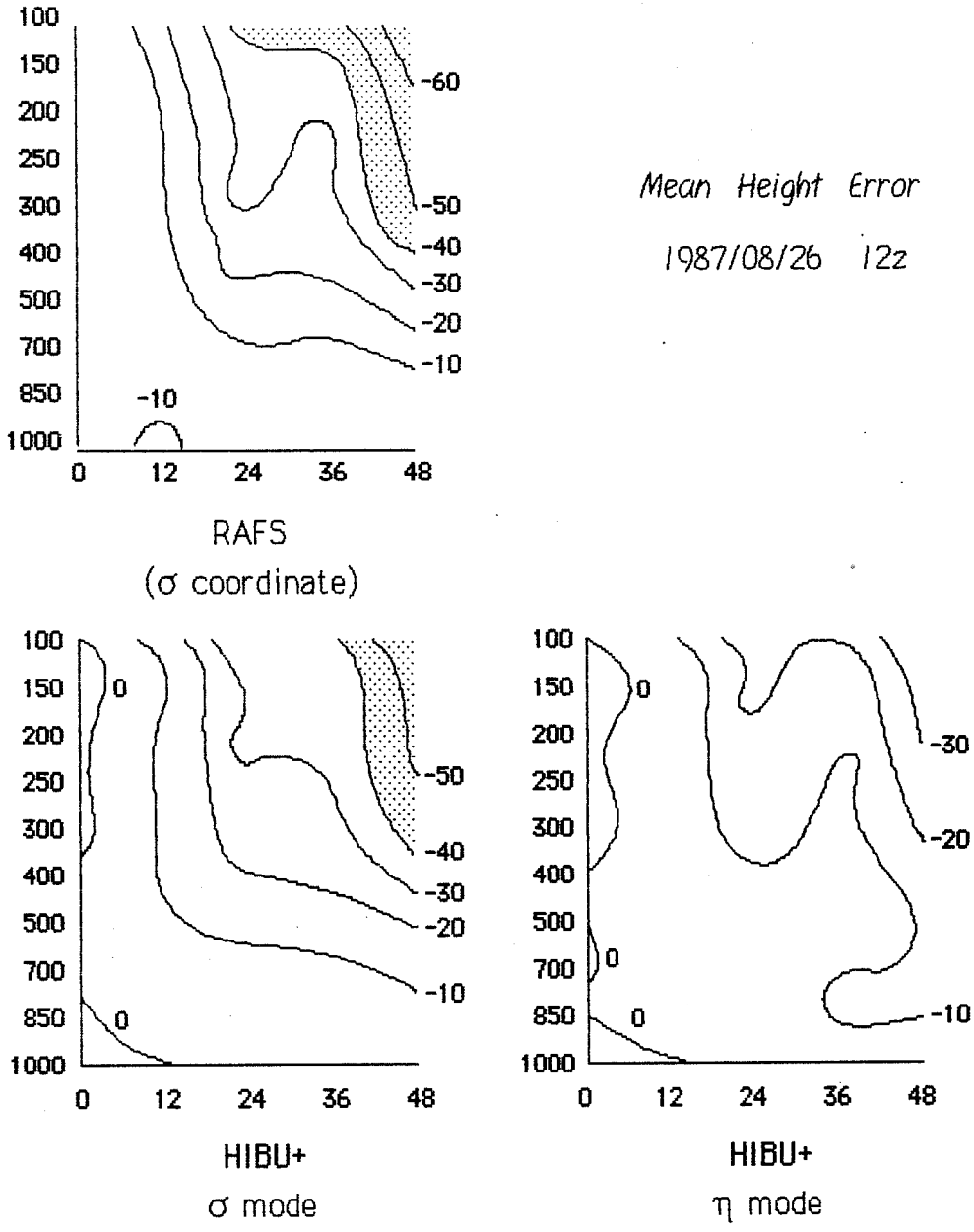

Fig. III.3. Same as Fig. III.2 but for August 26, 1987, 12Z.

IV. Conclusions

IV.1. Small sacle forcing on the grids B/E and the grid C

Experiments with small scale forcing have been performed on the staggered grid C and on the semi-staggered grid E with a simple shallow-water model. The resolution has been varied in order to examine the convergence of the solutions, and, if the convergence were to be established,

to assess the rate of convergence on the two grids.

With forcing by a source and by a sink at single grid points, substantial difference between the solutions on the E and on the C grid has been demonstrated. Considering the depth at the sink, however, the solutions on the two grids have been found to converge toward the same value as the resolution is increased.

With modest weight of the modification (Mesinger 1973; Janjić 1979), the solution on the E grid approaches the true solution with about equal rapidity as that on the C grid. However, the C grid tends to underestimate the amplitude of the disturbance, while the reverse is true on the E grid. Thus, the solutions on the two grids converge from different sides. This result is consistent with what should be expected from the geostrophic adjustment theory applied to the spatially discretized systems.

A disturbing implication is that different intensity of forcing may be required in order to produce the same effect depending on the grid choice.

It has been demonstrated that, in the set-up of the present experiments, the convergence properties of the E grid can be considerably improved by increasing the weight of the modification, with no penalty in terms of the economy of the computation.

IV.2. Forcing due to topography and the vertical coordinate

The choice of the vertical coordinate is relevant for the horizontal discretization because of possible considerations concerning the treatment of internal boundaries. An example requiring such considerations is the step-mountain η coordinate (Mesinger, 1984; Mesinger et al., 1987).

The most popular σ coordinate is a special case of the η coordinate. Thus, a model formulated in the η coordinate can be run in the σ coordinate. This feature of the η coordinate was used in a series of numerical experiments with the HIBU model (Mesinger et al., 1987; Janjić and Black, 1987) in order to assess the relative advantages and disadvantages of the two techniques for representation of mountains.

In the early experiments with the "minimum physics" version of the model (Mesinger, 1985), it was noticed that when the model was run in the σ mode a much higher level of noise was produced than in the η mode. This remained generally true as the new physical parameterization schemes were

being incorporated in the model.

The HIBU+ model with a comprehensive physical package was used in a recent series of 13 consecutive 48 hour forecasts (Black and Janjić, 1988).

Considerably better threat scores for precipitation were obtained in the η mode. On the other hand, the bias scores were generally better in the σ mode. However, the representativeness of this result is not quite clear having in mind the inconsistencies in the reinterpolations involved in the verification procedure.

On the average, the mean height error in the σ mode was considerable at the end of the 48 hour forecast period, and generally about twice larger than that of the η mode. The mean height error of another reference σ coordinate model, with resolution similar to that of the HIBU+ model, was even larger than that of the HIBU+ model run in the σ mode, and in some individual cases the error patterns showed striking similarity to those of the HIBU+ σ mode runs.

These results suggest that the σ coordinate is responsible for the large mean height errors. Although the sample considered is relatively short, the sensitivity of the HIBU+ model to changing the vertical coordinate from σ to η was strong and systematic. This result was, in a way, reconfirmed by comparison with another σ coordinate model which was very different from the HIBU+ model. The exact mechanism of the error growth in the σ coordinate remains unknown.

Acknowledgements: This research was supported by the Serbian Academy of Sciences and Arts, and by the University Corporation for Atmospheric Research under contract No. 9523. The experiments with full physics model reported here were performed using the data and the computer facilities of the National Meteorological Center, Washington.

REFERENCES

Arakawa, A., 1970: Numerical simulation of large-scale atmospheric motions. Numerical Solution of Field Problems in Continuum Physics, Vol. 2, SIAM-AMS Proceedings, G. Birkhoff and S. Varga, Eds., Amer. Math. Soc., 24-40.

Arakawa, A., 1972: Design of the UCLA general circulation model. Numerical Simulation of Weather and Climate, Tech. Rep. No. 7, Dept. Meteor., UCLA, Los Angeles.

Arakawa, A. and V.R. Lamb, 1977: Computational design of the basic dynamical processes of the UCLA general circulation model. Methods in Computational Physics, Vol. 17, Academic Press, 173-265.

Arakawa, A. and V.R. Lamb, 1981: A potential enstrophy and energy conserving scheme for the shallow water equations. Mon. Wea. Rev., **109**, 18-36.

Betts, A.K., 1986: A new convective adjustment scheme. Part I: Observational and theoretical basis. Quart. J. R. Met. Soc., **112**, 677-691.

Betts, A.K. and M.J. Miller, 1986: A new convective adjustment scheme. Part II: Single column tests using GATE wave, BOMEX, ATEX and Arctic Air-mass data sets. Quart. J. R. Met. Soc., **112**, 693-709.

Black, T.L and Z.I. Janjić, 1988: Preliminary forecast results from a step-mountain eta coordinate regional model. To be presented at the Eighth Conf. Numerical Weather Prediction, Baltimore, Amer. Meteor. Soc.

Cullen, M.J.P., 1983: Current progress and prospects in numerical techniques for weather prediction models. J. Comp. Phys., **50**, 1-37.

Daley, R., 1980: On the optimal specification of the initial state for deterministic forecasting. Mon. Wea. Rev., **108**, 1719-1735.

Davies, R., 1982: Documentation of the solar radiation parameterization in the GLAS climate model. NASA Tech. Memo. 83961, 57 pp.

Dragosavac, M. and Z.I. Janjić, 1987: Stationary solutions of linearized shallow water equations induced by topography on various grids. Mon. Wea. Rev., **115**, 730-736.

Harshvardhan and D.G. Corsetti, 1984: Longwave radiation parameterization for the UCLA/GLAS GCM. NASA Tech. Memo. 86072, 48 pp.

Janjić, Z. I., 1974: A stable centered difference scheme free of two-grid-interval noise. Mon. Wea. Rev., **102**, 319-323.

Janjić, Z. I., 1979: Forward-backward scheme modified to prevent two-grid-interval noise and its application in sigma coordinate models. Contrib. Atmos. Phys., **52**, 69-84.

Janjić, Z. I., 1984: Non-linear advection schemes and energy cascade on semi-staggered grids. Mon. Wea. Rev., **112**, 1234-1245.

Janjić, Z.I. and T.L. Black, 1987: Physical package for the step-mountain, eta coordinate model. Submitted to: Research Activities in Atmospheric and Oceanic Modelling, WCRP, No. 10.

Janjić, Z. I. and F. Mesinger, 1984: Finite-difference methods for the shallow water equations on various horizontal grids. Numerical Methods for Weather Prediction, Seminar 1983, Vol. 1, ECMWF, Reading, U.K., 29-101.

Janjić, Z. I. and A. Wiin-Nielsen, 1977: On geostrophic adjustment and numerical procedures in a rotating fluid. J. Atmos. Sci., **34**, 297-310.

Mellor, G.L. and T. Yamada, 1974: A hierarchy of Turbulence closure models for planetary boundary layers. J. Atmos. Sci., **31**, 1791-1806.

Mellor, G.L. and T. Yamada, 1982: Development of a turbulence closure model for geophysical fluid problems. Rev. Geophys. Space Phys., **20**, 851-875.

Mesinger, F., 1973: A method for construction of second-order accuracy difference schemes permitting no false two-grid-interval wave in the height field. Tellus, **25**,44-458.

Mesinger, F., 1974: An economical explicit scheme which inherently prevents the false two-grid interval wave in the forecast fields. Proc. Symp. on Difference and Spectral Methods for Atmosphere and Ocean Dynamics Problems, Novosibirsk, 17-22 September 1973, Acad. Sci., Novosibirsk, Part II, 18-34.

Mesinger, F., 1981: Horizontal advection schemes of a staggered grid - an enstrophy and energy-conserving model. Mon. Wea. Rev., **109**, 467-478.

Mesinger, F., 1984: A blocking technique for representation of mountains in atmospheric models. Riv. Meteor. Aeronautica, **44**, 195-202.

Mesinger, F., 1985: The sigma system problem. Preprints, Seventh Conf. Numerical Weather Prediction, Montreal, Amer. Meteor. Soc., 340-347.

Mesinger, F. and Z.I. Janjić, 1987: Numerical technique for the representation of mountains. In: Observation, Theory and Modelling of Orographic Effects, Seminar 1986, Vol. 2, ECMWF, Reading, U.K. (in press).

Mesinger, F., Z.I. Janjić, S. Ničković, D. Gavrilov, and D.G. Deaven, 1987: The step-mountain coordinate: model description and performance for cases of Alpine lee cyclogenesis and for a case of an Appalachian redevelopment. Submitted to Mon. Wea. Rev.

Vasiljević, D., 1982: The effect of MESINGER's procedure for preventing grid separation on the geostrophic mode. Contrib. Atmos. Phys., **55**, 177-181.

Winninghoff, F. J., 1968: On the adjustment toward a geostrophic balance in a simple primitive equation model with application to the problems of initialization and objective analysis. Ph. D. Thesis, Dept. Meteor., UCLA, Los Angeles.

Zilitinkevitch, S.S., 1970: Dynamics of the planetary boundary layer. Gidro-meteorologicheskoe Izdatelystvo, Leningrad, 292 pp (in Russian).